

# Di- $\pi^0$ correlations in $p+p$ , $p+Al$ and $p+Au$ collisions at $\sqrt{s_{NN}} = 200$ GeV at STAR

Xiaoxuan Chu<sup>1</sup>,  
for the STAR Collaboration

1 Brookhaven National Laboratory, Upton, New York 11973, USA  
\* xchu@bnl.gov

July 29, 2021



*Proceedings for the XXVIII International Workshop  
on Deep-Inelastic Scattering and Related Subjects,  
Stony Brook University, New York, USA, 12-16 April 2021  
doi:10.21468/SciPostPhysProc.?*

## Abstract

The STAR Collaboration reports measurements of back-to-back azimuthal correlations of di- $\pi^0$  produced at forward pseudorapidity ( $2.6 < \eta < 4.0$ ) in  $p+p$ ,  $p+Al$  and  $p+Au$  collisions at a center-of-mass energy per nucleon-nucleon pair of 200 GeV. A clear suppression of the correlated away-side yields is observed in  $p+Au$  and for the first time in  $p+Al$  collisions, compared with the  $p+p$  data. The enhanced suppression found in  $p+Au$  with respect to  $p+Al$  collisions exhibits the saturation scale ( $Q_s^2$ ) dependence on the mass number  $A$ . The observed suppression of back-to-back pairs as a function of event activity and transverse momentum points to non-linear gluon dynamics arising at high parton densities.

## 1 Introduction

Collisions between hadronic systems, i.e.,  $p+A$  and  $d+A$  at the Relativistic Heavy Ion Collider (RHIC) provide a window to the parton distributions of nuclei at small momentum fraction ( $x$ ). Several RHIC measurements [1–5] have shown that the hadron yields at forward rapidities (deuteron going direction) are suppressed in  $d+Au$  collisions relative to  $p+p$  collisions at  $\sqrt{s_{NN}} = 200$  GeV. Possible mechanisms leading to the suppression include gluon saturation [6] and energy loss [7, 8]. Meanwhile, the contributions from double-parton interactions to the  $d+A \rightarrow \pi^0 \pi^0 X$  cross section are suggested as an alternative explanation of the suppression [9]. Therefore, it is important to carry out the same measurement in  $p+A$  collisions, which are theoretically and experimentally cleaner compared to  $d+A$  collisions.

The density of gluons per unit transverse area is expected to be larger in nuclei than in nucleons at a given  $x$ ; thus, nuclei provide a natural environment to study non-linear gluon evolution. Gluons from different nucleons can interfere and amplify the total transverse gluon density by a factor of  $A^{1/3}$  for a nucleus with mass number  $A$ . The color glass condensate (CGC) framework [10, 11] predicts that a quark or gluon scattering at forward angles (large rapidities) will interact coherently with gluons at low- $x$  in the nucleus [12]. As a result, for di-hadron correlations on the away-side, the yield of associated hadrons is expected to be suppressed and the correlation peak is predicted to be broadened in  $p(d)+A$  collisions compared to  $p+p$  collisions [13, 14].

In this contribution, we report measurements of back-to-back di- $\pi^0$  correlations for  $p$ +Al and  $p$ +Au collisions relative to  $p$ + $p$  collisions in the forward-rapidity region ( $2.6 < \eta < 4.0$ ) at  $\sqrt{s_{\text{NN}}} = 200$  GeV. The use of different ion beams provides an opportunity to study the saturation scale ( $Q_s^2$ ) dependence on  $A$ . The correlation function  $C(\Delta\phi) = N_{\text{pair}}(\Delta\phi)/(N_{\text{trig}} \times \Delta\phi)$  is measured, where  $N_{\text{pair}}$  is the yield of the correlated trigger and associated  $\pi^0$  pairs,  $N_{\text{trig}}$  is the trigger  $\pi^0$  yield,  $\Delta\phi$  is the azimuthal angle difference between the trigger and associated  $\pi^0$ . In each pair, trigger  $\pi^0$  is the one with higher transverse momentum  $p_T$  ( $p_T^{\text{trig}}$ ); associated  $\pi^0$  is the one with lower  $p_T$  ( $p_T^{\text{asso}}$ ). To remove detector acceptance effects, the measured correlation functions are divided by the correlation functions from mixed events.

## 2 Experiment and Dataset

Datasets for  $p$ + $p$ ,  $p$ +Al and  $p$ +Au collisions were recorded in 2015. The  $\pi^0$ s were reconstructed from photons, which were identified with the STAR forward meson spectrometer (FMS). The FMS is an electromagnetic calorimeter covering a pseudorapidity range from 2.6 to 4.0 [15]. The collision events are triggered by FMS based on the transverse energy deposition. The  $p$ +Al and  $p$ +Au samples are separated into different event activity (E.A.) classes based on the energy ( $\Sigma E_{\text{BBC}}$ ) deposited in the inner sectors of the beam beam counter (BBC) at backward direction (aluminum and gold going direction,  $3.3 < -\eta < 5.0$ ), where  $\Sigma E_{\text{BBC}}$  is the ADC sum from all 16 BBC tiles. The STAR BBC is a scintillator detector which measures minimum-ionizing particles [16]. The samples without any E.A. selections are minimum bias (MinBias) data. The energy and  $p_T$  of the photon candidates are required to be above 1 GeV and 0.1 GeV/ $c$ , respectively. The reconstructed  $\pi^0$ 's  $p_T$  is above 0.5 GeV/ $c$ . The energy asymmetry of  $\pi^0$ 's photon components  $|\frac{E_1 - E_2}{E_1 + E_2}|$  is required to be below 0.7, where  $E_1$  and  $E_2$  are the photon energies. The selected mass range of the  $\pi^0$  candidates is between 0.07 and 0.2 GeV/ $c^2$ .

## 3 Results

The corrected correlation function as described in Sec. 1 is fitted with two individual Gaussians at the near- ( $\Delta\phi = 0$ ) and away-side ( $\Delta\phi = \pi$ ) peaks, together with a constant for the pedestal, from  $\Delta\phi = -\pi/2$  to  $\Delta\phi = 3\pi/2$ . The near-side peak, dominated by two  $\pi^0$ s coming from the same jet, encodes nuclear modifications to the parton fragmentation. This proceeding will not discuss the near-side physics, and focuses on the study of the away-side peak. The area of the away-side peak is the integral of the correlation function from  $\Delta\phi = \pi/2$  to  $\Delta\phi = 3\pi/2$  after pedestal subtraction, representing the back-to-back  $\pi^0$  yields per trigger particle; the corresponding width is defined as the  $\sigma$  of the away-side peak according to the fit.

Figure 1 shows the comparison of forward back-to-back di- $\pi^0$  correlation function in Min-Bias  $p$ + $p$ ,  $p$ +Al and  $p$ +Au collisions at  $\sqrt{s_{\text{NN}}} = 200$  GeV. The area and width of away-side peak from different collisions are shown, together with their statistical uncertainties. In the left panel, in the low  $p_T$  regime, a clear suppression is observed in  $p$ +A compared to the  $p$ + $p$  data. The away-side associated  $\pi^0$  yield per-trigger in  $p$ +Au ( $p$ +Al) is suppressed by about a factor 1.7 (1.2) with respect to  $p$ + $p$  collisions. The enhanced suppression in  $p$ +Au relative to  $p$ +Al at the same collision energy supports an  $A$  dependence of  $Q_s^2$  as predicted in [10, 13]. The suppression decreases with increasing  $p_T$  of the  $\pi^0$ s. In the high  $p_T$  range, no suppression is observed in  $p$ +A compared to  $p$ + $p$  collisions as can be seen in the right panel of Fig. 1. The parton momentum fraction  $x$  with respect to the nucleon inside the nucleus increases with the

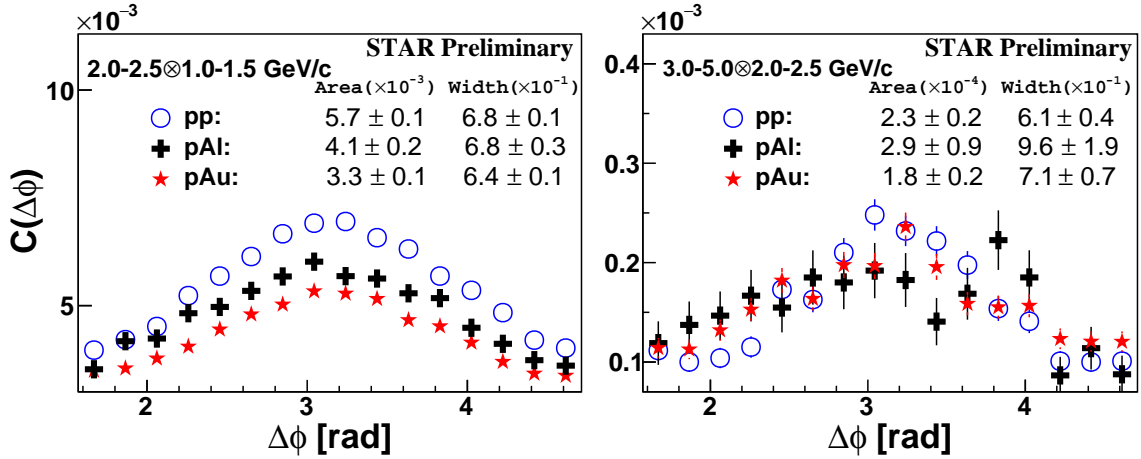


Figure 1: Comparison of the correlation functions vs. azimuthal angle difference between forward ( $2.6 < \eta < 4.0$ )  $\pi^0$  pairs in MinBias  $p+p$ ,  $p+Al$  and  $p+Au$  collisions at  $\sqrt{s_{NN}} = 200$  GeV. Left panel: the trigger  $\pi^0$ 's  $p_T$  ( $p_T^{\text{trig}}$ ) = 2–2.5 GeV/c and the associated  $\pi^0$ 's  $p_T$  ( $p_T^{\text{asso}}$ ) = 1–1.5 GeV/c; right panel:  $p_T^{\text{trig}} = 3$ –5 GeV/c and  $p_T^{\text{asso}} = 2$ –2.5 GeV/c. The area and width of away-side peaks are shown in each panel as described in the text.

$p_T$  of the trigger and associated  $\pi^0$ s.  $Q$  can be approximated as the average  $p_T$  of di- $\pi^0$ . The low  $x$  and  $Q^2$  regime, where the gluon density is large and expected to be saturated, can be accessed using low  $p_T$  di- $\pi^0$  pairs. When the  $\pi^0$   $p_T$  is high, the probed  $x$  ( $Q^2$ ) will not be sufficiently small to reach a non-linear regime. The phenomenon of broadening is not observed in  $p+A$  collisions, which is consistent with the similar measurement in  $d+Au$  collisions by the PHENIX experiment [5].

In Fig. 2, ratios of the away-side peak area for di- $\pi^0$  correlations from  $p+Al$  and  $p+Au$  collisions to that from MinBias  $p+p$  collisions are shown for different event activity classes. The systematic uncertainties of the area arise from non-uniform detector efficiency as a function of  $\phi$ , and estimated as the following. We started with a physical-like correlation without detector effects. A correlation with detector effects included was obtained by applying weights according to the  $\phi$  distributions from data, and then a mixed event correction was applied to the correlation as done in real data analysis. The difference between the input physical-like

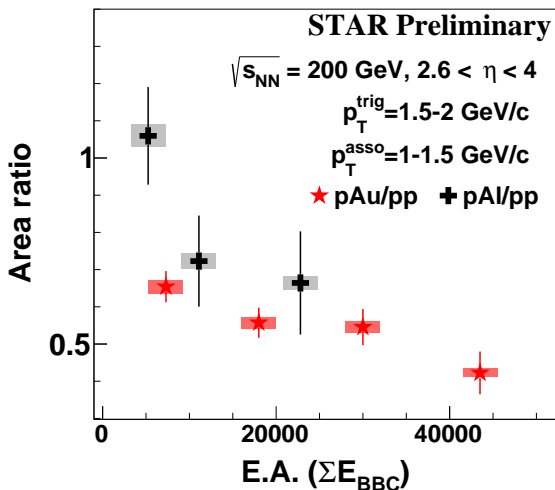


Figure 2: Area ratio of away-side di- $\pi^0$  correlation at forward rapidities ( $2.6 < \eta < 4.0$ ) for different event activity bins from  $p+Al$  and  $p+Au$  relative to MinBias  $p+p$  collisions at  $p_T^{\text{trig}} = 1.5$ –2 GeV/c and  $p_T^{\text{asso}} = 1$ –1.5 GeV/c. The vertical bars around each data point indicate statistical uncertainties and the vertical bands indicate point-to-point systematic uncertainties. The width of the band is chosen for visibility and doesn't reflect uncertainties.

and the corrected correlation is taken as the systematic uncertainty. An enhanced suppression in high activity events is observed in  $p$ +Au and  $p$ +Al data, and the significance of the stronger suppression in the highest E.A. than the lowest E.A. in  $p$ +Au ( $p$ +Al) collisions is 3.1 (1.7)  $\sigma$ . Less suppression is observed in  $p$ +Al compared to  $p$ +Au, which is consistent with the results at low  $p_T$  from MinBias  $p$ +Al and  $p$ +Au data shown in the left panel of Fig. 1.

## 4 Conclusion

In summary, measurements of azimuthal correlations of  $\text{di-}\pi^0$  at forward rapidities ( $2.6 < \eta < 4.0$ ) are performed using 2015 200 GeV  $p$ + $p$ ,  $p$ +Al and  $p$ +Au data at STAR. A clear suppression of away-side yields is observed in  $p$ +A in comparison with  $p$ + $p$  collisions at low  $p_T$ . The suppression is enhanced at higher E.A. and for pairs probing smaller  $x$  (and  $Q^2$ ) with lower  $\text{di-}\pi^0$ 's  $p_T$ . No increase in the width of the azimuthal angular correlation is seen within experimental uncertainties. The presented results are the first measurement of the nuclear effect dependence on  $A$ , where we observe that the suppression is enhanced with larger  $A$ .

## 5 Acknowledgements

We thank the RHIC Operations Group and RCF at BNL. This work is supported by U.S. Department of Energy under contract number de-sc0012704.

## References

- [1] I. Arsene *et al.*, *Transverse momentum spectra in Au+Au and d+Au collisions at  $\sqrt{s_{NN}} = 200$  GeV and the pseudorapidity dependence of high  $p(T)$  suppression*, Phys. Rev. Lett. **91**, 072305 (2003), doi:[10.1103/PhysRevLett.91.072305](https://doi.org/10.1103/PhysRevLett.91.072305).
- [2] I. Arsene *et al.*, *On the evolution of the nuclear modification factors with rapidity and centrality in d+Au collisions at  $\sqrt{s_{NN}} = 200$  GeV*, Phys. Rev. Lett. **93**, 242303 (2004), doi:[10.1103/PhysRevLett.93.242303](https://doi.org/10.1103/PhysRevLett.93.242303).
- [3] S. S. Adler *et al.*, *Nuclear modification factors for hadrons at forward and backward rapidities in d+Au collisions at  $\sqrt{s_{NN}} = 200$  GeV*, Phys. Rev. Lett. **94**, 082302 (2005), doi:[10.1103/PhysRevLett.94.082302](https://doi.org/10.1103/PhysRevLett.94.082302).
- [4] J. Adams *et al.*, *Forward neutral pion production in  $p$ + $p$  and  $d$ +Au collisions at  $\sqrt{s_{NN}} = 200$  GeV*, Phys. Rev. Lett. **97**, 152302 (2006), doi:[10.1103/PhysRevLett.97.152302](https://doi.org/10.1103/PhysRevLett.97.152302).
- [5] A. Adare *et al.*, *Suppression of back-to-back hadron pairs at forward rapidity in  $d$ +Au collisions at  $\sqrt{s_{NN}} = 200$  GeV*, Phys. Rev. Lett. **107**, 172301 (2011), doi:[10.1103/PhysRevLett.107.172301](https://doi.org/10.1103/PhysRevLett.107.172301).
- [6] L. V. Gribov, E. M. Levin and M. G. Ryskin, *Semihard Processes in QCD*, Phys. Rept. **100**, 1 (1983), doi:[10.1016/0370-1573\(83\)90022-4](https://doi.org/10.1016/0370-1573(83)90022-4).
- [7] I. Vitev, *Non-Abelian energy loss in cold nuclear matter*, Phys. Rev. C **75**, 064906 (2007), doi:[10.1103/PhysRevC.75.064906](https://doi.org/10.1103/PhysRevC.75.064906).
- [8] Z.-B. Kang, I. Vitev and H. Xing, *Dihadron momentum imbalance and correlations in  $d$ +Au collisions*, Phys. Rev. D **85**, 054024 (2012), doi:[10.1103/PhysRevD.85.054024](https://doi.org/10.1103/PhysRevD.85.054024).

- [9] M. Strikman and W. Vogelsang, *Multiple parton interactions and forward double pion production in pp and dA scattering*, Phys. Rev. D **83**, 034029 (2011), doi:[10.1103/PhysRevD.83.034029](https://doi.org/10.1103/PhysRevD.83.034029).
- [10] L. D. McLerran and R. Venugopalan, *Computing quark and gluon distribution functions for very large nuclei*, Phys. Rev. D **49**, 2233 (1994), doi:[10.1103/PhysRevD.49.2233](https://doi.org/10.1103/PhysRevD.49.2233).
- [11] L. D. McLerran and R. Venugopalan, *Gluon distribution functions for very large nuclei at small transverse momentum*, Phys. Rev. D **49**, 3352 (1994), doi:[10.1103/PhysRevD.49.3352](https://doi.org/10.1103/PhysRevD.49.3352).
- [12] V. Guzey, M. Strikman and W. Vogelsang, *Observations on dA scattering at forward rapidities*, Phys. Lett. B **603**, 173 (2004), doi:[10.1016/j.physletb.2004.10.033](https://doi.org/10.1016/j.physletb.2004.10.033).
- [13] D. Kharzeev, E. Levin and L. McLerran, *Jet azimuthal correlations and parton saturation in the color glass condensate*, Nucl. Phys. A **748**, 627 (2005), doi:[10.1016/j.nuclphysa.2004.10.031](https://doi.org/10.1016/j.nuclphysa.2004.10.031).
- [14] C. Marquet, *Forward inclusive dijet production and azimuthal correlations in p(A) collisions*, Nucl. Phys. A **796**, 41 (2007), doi:[10.1016/j.nuclphysa.2007.09.001](https://doi.org/10.1016/j.nuclphysa.2007.09.001).
- [15] J. Adam *et al.*, *Longitudinal Double-Spin Asymmetries for  $\pi^0$ s in the Forward Direction for 510 GeV Polarized pp Collisions*, Phys. Rev. D **98**(3), 032013 (2018), doi:[10.1103/PhysRevD.98.032013](https://doi.org/10.1103/PhysRevD.98.032013).
- [16] C. A. Whitten, *The beam-beam counter: A local polarimeter at STAR*, AIP Conf. Proc. **980**(1), 390 (2008), doi:[10.1063/1.2888113](https://doi.org/10.1063/1.2888113).
- [17] J. Adam *et al.*, *Comparison of transverse single-spin asymmetries for forward  $\pi^0$  production in polarized pp, pAl and pAu collisions at nucleon pair c.m. energy  $\sqrt{s_{NN}} = 200$  GeV*, Phys. Rev. D **103**(7), 072005 (2021), doi:[10.1103/PhysRevD.103.072005](https://doi.org/10.1103/PhysRevD.103.072005).
- [18] J. Adam *et al.*, *Measurement of transverse single-spin asymmetries of  $\pi^0$  and electromagnetic jets at forward rapidity in 200 and 500 GeV transversely polarized proton-proton collisions*, Phys. Rev. D **103**(9), 092009 (2021), doi:[10.1103/PhysRevD.103.092009](https://doi.org/10.1103/PhysRevD.103.092009).